Appl. Chem. Eng., Vol. 25, No. 1, February 2014, 107-112
http://dx.doi.org/10.14478/ace.2013.1106

Short communication

과산화수소 정량을 위한 장미조직 함유 바이오센서의 전기화학 속도론적 고찰

유근배†

청주대학교 응용화학과
(2013년 9월 30일 접수, 2013년 11월 1일 심사, 2013년 12월 11일 채택)

Electrochemical Kinetic Assessment of Rose Tissue Immobilized Biosensor for the Determination of Hydrogen Peroxide

Keun-Bae Rhyu†

Department of Applied Chemistry, Cheongju University, Cheongju 360-764, Korea
(Received September 30, 2013; Revised November 1, 2013; Accepted December 11, 2013)

흑연가루의 결합재로 클로로술폰화 폴리에틸렌 고무용액을, 매개체로 ferrocene을 사용하여 장미조직을 고정한 과산화수소 정량 바이오센서를 제작하였다. 실험 전극전위 영역에서 보여준 Hanes-Woolf 도시의 선형성은 기질의 환원이 장미 과산화효소의 촉매력에 의한 것임을 보여 주었다. 또 얻어진 10개 이상의 전기화학 파라미터들은 전극이 정량적으로 성능을 발휘하고 있음을 입증하였다. 이런 사실들은 효소전극의 실용화를 위하여 장미조직이 상업용 과산화효소를 대치하여 사용될 수 있음을 확신시켜 주는 것이었다.

Using a chlorosulphonated polyethylene rubber solution for a binder of graphite powder and ferrocene for a mediator, a rose leaf tissue-embedded biosensor was built. Linearity on the Hanes-Woolf plot showed the reduction of the substrate was attained through the catalytic power of the rose peroxidase in the experimental range of electrode potential. Furthermore, 10 or more electrochemical parameters demonstrated that the electrode exerts its sensing ability quantitatively. The foregoing gave the full conviction that rose tissue can be used in place of the currently marketed enzyme for the practical use of enzyme electrode.

Keywords: *biosensor, enzyme electrode, peroxidase, hydrogen peroxide*

1. Introduction

Speedy and quantitative determination of hydrogen peroxide is very important in various fields and industries including electroplating, sewage purification, rocket propulsion, chemical synthesis and others[1]. Though there are various classical methodologies to assay hydrogen peroxide, the spectroscopic and the electrochemical method are currently the most common approaches[2-4]. The spectroscopic method is based on luminescence which gives a particular prominence to determine detection limits from the matrix but requires both costly and time-consuming procedures. In cases where hypersensitiveness is not required for measurements, those procedures are easily reduced with electrochemical sensors[5-7].

Immense catalytic power and specificity are the most striking characteristics of enzymes. The two mentioned above are applicable to the quantitative analyses. The functioning principle of the enzyme electrode can be summarized as follows. The active site of enzyme is 3-dimensional and situated deep within the enzyme protein. As it is some distance from the electrode surface, a considerable overvoltage is required to initiate the redox reaction at its location. This may be the immediate cause of the side reactions. To eliminate the possibility of the systematic noises of this kind, a mediator, which transfers electrons from the electrode to the active site at the low electrode potential, is employed. The signal resulting from this effort is free from possible reactions.

The application of the principle has been varied. Several of the applications are as follows : carbon paste method[8], screen-printing[9], functionalized sol-gel techniques[10], entrapping enzyme in polypyrrole films[11], immobilization by physical adsorption[12] and such like. The carbon paste method is a rapid and simple procedure to encapsulate enzyme in electrode materials and there has been increasing attention on the development of carbon paste electrode using rubber solution as a binder of graphite powder in this lab.

There have been numerous instances where plant or animal tissue

† Corresponding Author: Cheongju University
Department of Applied Chemistry
#298 Daeseong-ro, Sangdang-gu, Cheongju 360-764, Korea
Tel: +82-43-229-8537 e-mail: krhyu@cju.ac.kr

pISSN: 1225-0112 @ 2014 The Korean Society of Industrial and Engineering Chemistry.

was embedded in carbon paste as a zymogen to construct the enzyme electrode[13-15]. For example, the marketed peroxidase extracted from horseradish was used to decrease noise and to increase electrical signal. Although the expected results were achieved, its high cost prevented biosensors from wide commercial use.

In an effort to overcome those complications, efforts to find the zymogen in all spheres of daily life have been made by this lab[16-20]. This paper extends those efforts. Below is described the electrochemical behaviors of the rose electrode designed in hope that this electrode will sufficiently meet the criteria mentioned above. In fact, the result did meet our expectations and its details are reported below.

2. Experiments

2.1. Reagents and Instruments

Rose leaf was used as a zymogen and the term 'the rose electrode' is given to the new electrode covering the paper. Chlorosulphonated polyethylene rubber (abbr. CSPR, Denki Kagaku Kogyo Kabushiki kaisha Mitsui Co.) solution was a binder of graphite powder. Toluene (Sigma-Aldrich, ≥ 99.9%) was used for liquefying rubber, ferrocene (Sigma, F-3375, USA) for a mediator and graphite powder (≤ 0.1 mm, Fluka, Switzerland) for electrode material was used without alteration. The substrate and the electrolyte were hydrogen peroxide (Junsei, EP, 35%) and NaCl (Shinyo pure Chem. ≥ 99.5%), respectively. A BAS Model EPSILON (Bioanalytical System, Inc., U. S. A.) was employed for cyclic voltammograms (CV) and EG&G Model 362 (Princeton Applied Research), for other signals. The reference electrode and the auxiliary electrode were Ag/AgCl (BAS MF 2052) and Pt electrode (BAS MW 1032), respectively.

2.2. Construction of Enzyme Electrode

The fabricating procedure of the rose electrode is as follows: the homogeneous mixture of 0.91 g of graphite powder and ferrocene solution (0.09 g in 10 mL of $CHCl_3$) was dried in a mild condition. The electrode material was produced by mixing 1.0 g of the ferrocene coated powder with the CSPR solution (1.5%) at a 1 : 1 ratio (wt/wt). 1 g of this paste was completely mixed with 0.20 g of the ruptured rose leaf tissue. The biosensor was completed by packing this paste into a 7 mm i. d. and a 2 mm deep polyethylene tube with an ohmic contact[21].

3. Results and Discussion

Figure 1 displays four segment CV clarifying the electrochemical behaviors of the rose electrode in the stirred 0.1 M NaCl solution without Figure 1(a) and with Figure 1(b) substrate (2.0×10^{-2} M H_2O_2). Voltammogram Figure 1(a) obtained for the background solution shows the increasing of the residual current over potential. Constituents of this system are water, graphite powder for the conductor, CSPR for the binder, ferrocene for the mediator, and rose tissue. The standard reduction potential of water is -0.828 V and of ferricinium ion is +0.400 V in this system. It would be especially

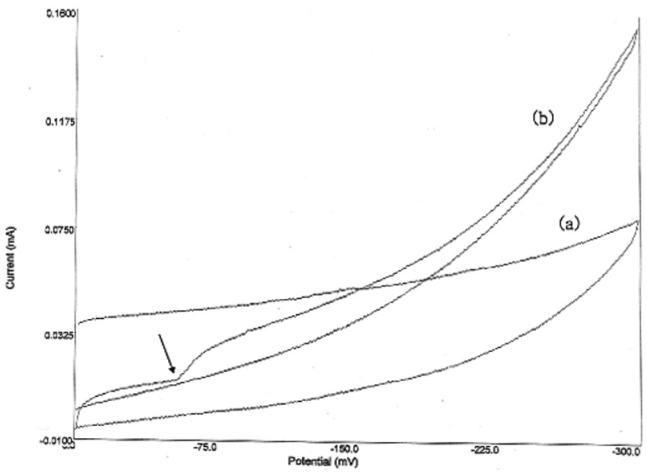

Figure 1. Four segment cyclic voltammogram showing the sensing ability of the electrode for hydrogen peroxide in a stirred solution : (a) in the absence of H_2O_2 ; (b) in the presence of 2.0×10^{-2} M H_2O_2. Initial potential : 0 (mV) ; switching potential 1 : -300 (mV) ; switching potential 2 : 0 (mV) ; switching potential 3 : -300 (mV) ; final potential : 0 (mV) ; scan rate : 25 (mV/s). Arrow indicates the time of H_2O_2 addition.

cogent if the tails of the reduction function of water and ferricinium would not have any influence over our experimental range of potential. So it is very important that the background current Figure 1(a) bears no relation to the reduction of water and the mediator[22,23].

The binder, CSMR, is a chemical mixture consisting of chlorosulphonation brought about by the Reed-Horn reaction[24]. Though each component of the rubber has not been elucidated, residual current appearing in Figure 1(a) can be viewed as the reduction current of unidentified components in CSMR, or as the double layer charging current, considering that the signal in the forward scan is somewhat analogous in linearity. The fact that those are common to Figure 1(a) and 1(b) makes our approach reliable.

The cyclic voltammogram Figure 1(b) shows the process of electrolysis of the substrate when other conditions are the same as in (a) of Figure 1. We can find a drastic increasing of the signal current as soon as the substrate is added (arrow). It is easy to see that this drastic reform of the signal was caused by the reduction of the substrate because other conditions are the same as in Figure 1(a). Two experiments that are equivalent to Figure 1(a) and 1(b) were carried out to obtain linear sweep voltammograms (LSV) in the static solution. Figure 2 shows current difference between the two LSV's. It is a matter of general knowledge that the current profile (*i vs. E*) is sigmoidal, typically in cases where the electrochemical reaction is diffusion-controlled. Figure 2 is one small part of the full wave because the experimental range of the electrode potential is confined in narrow limits. The functional relationship between signal current and applied potential, which was performed by the Boltzmann fit, is in substance as follows :

$$i = -0.00023 + 0.973 / [1 + exp\{(E + 0.546) / 0.0812\}]$$

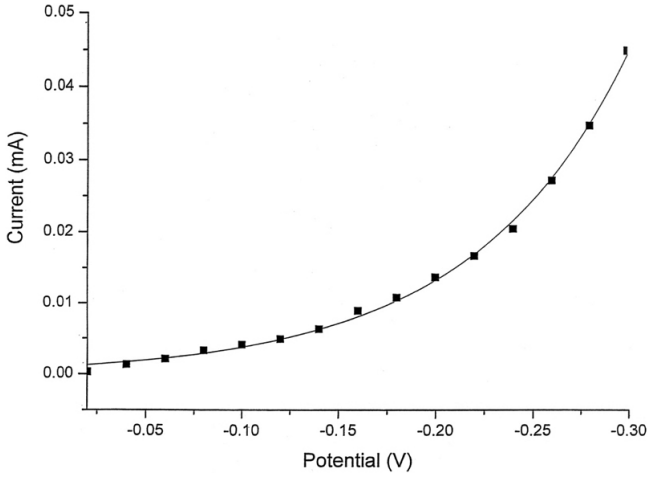

Figure 2. Potential dependence of current difference between (a) and (b) in a static solution. Other conditions are the same as in Figure 1 and the solid line corresponds to Boltzmann fitting (y = *-0.00023 + 0.97/(1 + exp(x + 0.55/0.08)*).

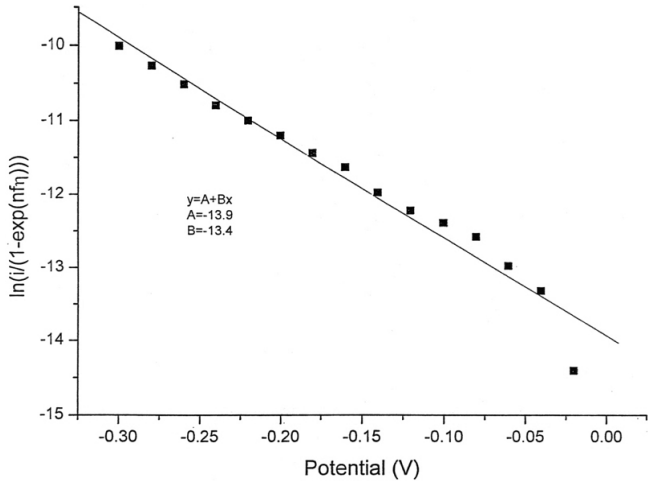

Figure 3. Tafel plot for cathodic branch of the signal current.

Where i is the current (mA) and E, the electrode potential (V). i is 0.973 mA at the negative infinity of the electrode potential, which is regarded as the limiting current ($i_{l.c}$) of our system (A = 0.38 cm^2, n = 1, *vide infra*). The above brings forth 1.33×10^{-4} cm/sec of mass transfer coefficient (m_o) and 26.4 Ω of mass transfer resistance (R_{mt}). As is well established, the reaction between ferrous iron and hydrogen peroxide in the organism is one electron transfer reaction (n = 1)[25-28]. In the irreversible system, the functional relation between the overpotential (η) and $\ln(i/(1-exp(nf\eta)))$ is linear. And its slope and intercept are αnf ($f=F/RT$) and $\ln i_o$ respectively. Figure 3 makes clear the above stated. The exchange current (i_o) and symmetry factor (α) worked out in Figure 3 are 9.19×10^{-7} A and 0.34, respectively. This symmetry factor is somewhat smaller than the numerical value typically found (0.5). This indicates that the reduction rate of the substrate is highly sensitive to the change of electrode potential. The passing of electrons between electrode and substrate is dependent on the characteristics of the double layer. The current transient of the rose

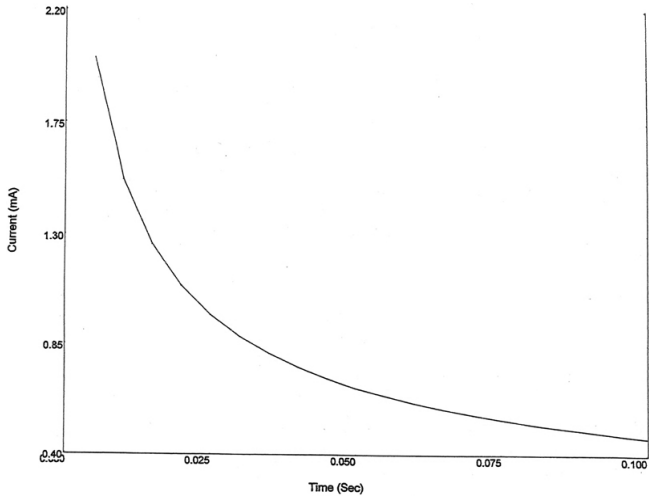

Figure 4. Transient of the double-layer charging current for a potential step in 0.1 M NaCl electrolytic solution. Start potential : 0 (mV); step potential : -300 (mV).

Table 1. Condenser Current Transients at Three Different Electrolyte Concentrations. *i* (mA) = *A1* × *exp*(-*t*/*t1*) + *i0*

-log[NaCl]	*A1*	*t1*	*i0*
1	1.91	0.015	0.59
2	0.25	0.031	0.30
3	0.014	0.035	0.068

electrode to gather information on the electrode-solution interface is given in Figure 4. It was obtained by the potential step technique at -300 mV in 0.10 M NaCl solution. In general, the condenser charging current decays in the fashion of the 1-st order exponential function, $i = (E/R_s)exp(-t/R_sC_d)$, where R_s and C_d are the solution resistance and the capacitance of the double layer, respectively. If the capacitor is assumed initially to be uncharged (q = 0 at t = 0), we obtain $i = E/R_s$ and $\tau = R_sC_d$. But Figure 4 makes it impossible to read the current at t = 0, as our measuring instrument is digitalized at the interval of 0.005 sec. The best way to bring a solution to this matter is to fit the currents obtained from 0.005 sec after potential excitation and to extrapolate its tendency to t = 0 sec. The relations between condenser current and time in this way are given in Table 1 at three different concentrations of electrolyte. In addition, $i_{t=0}$, R_s and many other parameters related are displayed in Table 2. Here time constant is the value for actual measurement. Table 2 shows the time constant increases with a low concentration of electrolyte. When applying a potential step of magnitude E, the charge on a capacitor as a function of the time is $q = EC[1 - exp(-t/R_sC)]$. Here the increase of time constant is traceable to the retardation of the double layer building with the increase of solution resistance. In addition, it indicates the calculated capacitance increases with a diluted concentration of electrolyte. The thickness of the diffusion layer is dependent on the concentration of ionic species in the solution, and the relation of capacitance to the thickness of the diffusion layer is $C = \varepsilon_0 \varepsilon A/d$, where A is the cross-sectional area of capacitor and d, the thickness.

Table 2. Electrode Parameters of the Biosensor

-log[NaCl]	$i_{t=0}$, mA	R_s, Ω	τ, sec	C, F	C_d, F	C_i, F
1	2.50	1.2×10^2	0.028	2.3×10^{-4}	1.2×10^4	$\fallingdotseq 2.3 \times 10^{-4}$
2	0.55	5.5×10^2	0.25	4.6×10^{-4}	3.9×10^3	$\fallingdotseq 4.6 \times 10^{-4}$
3	0.082	3.7×10^3	5.3	1.4×10^{-3}	1.2×10^3	$\fallingdotseq 1.4 \times 10^{-3}$

$i_{t=0}$: current at t = 0 sec; R_s : solution resistance; τ : time constant (obs); C : effective double layer capacitance; C_d : capacitance of the diffuse double layer; C_i : capacitance of the compact double layer.

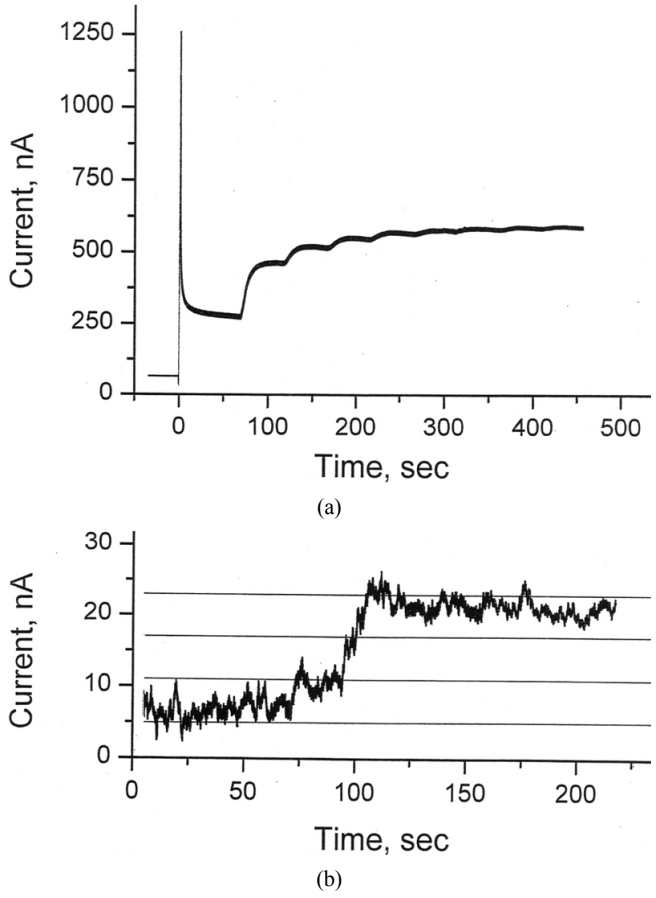

Figure 5. Time profiles of the signal current at -300 mV. (a) was caused by the successive increments of 50 μL of 0.1 M H_2O_2 and (b), by an addition of 40 μL of 0.01 M H_2O_2 for the determination of detection limit.

The rising tendency of capacitance mentioned above is attributable to the increase in the thickness of the double layer.

It is established that the capacitance (C_d) of the diffuse double layer is $228sqrt(c')cosh(19.47z\varphi)$ in the Gouy-Chapmann theory. The values in Table 2 are more or less higher than those (10～ 30 μF/cm^2) in theory. The value of capacitance becomes larger in proportion to the dielectric constant of the insulator. So the increase may be due to the large dielectric constant originated from rubber coating the graphite granule. Here an unequal relation, $C_d \gg C_i$, elicited from Table 2 means the effective capacitance of this system depends on the inner compact double layer.

Figure 5(a) is a typical amperogram obtained with the rose electrode while 50 μL of 0.10 M H_2O_2 is added successively at 50-second intervals into 10 mL of the stirred working solution.

This hydrodynamic amperometry has the advantages that a steady state of the faraday current is attained rather quickly because the mass transfer is much larger than that by diffusion. Also, the double layer charging current is shut out of the signal difference during before and after the addition of the substrate. A calibration curve, obtained from the accumulative signal currents and the accumulative substrate concentrations in Figure 5(a), is illustrated in the window of Figure 6.

Its prominent feature is that calibration deviates easily from the linearity even at low concentrations. This is usual with many other enzyme electrodes and several analyses are possible with these phenomena. First of all, the active sites on the electrode surface are limited in number and the intermediates may be adsorbed or saturated on the sensor surface to interfere with the mass transfer of substrate. Another account says that the enzyme can catalyze at any one of the steps when the dissociation of substrate goes through multi-step reactions. It was ascertained in this lab, experimentally that peroxidase extracted from horseradish (HRP) consists of two or more kinds of isozymes[29]. In case the rose electrode contains varieties of isozymes and they can take part in the dissociation of hydrogen peroxide at different rates, it remains as a possibility to explain the reason.

An amperogram for determining the detection limit of the electrode is in Figure 5(b). 40 μL of 0.01 M H_2O_2 was added to 10 mL of electrolyte solution at -300 mV. The detection limit was 4.5×10^{-5} M (S/N = 3) and it is similar to other limits[10,30-32]. Unless an extremely fast response is required, it will be elevated to a high degree as the disturbance of (b) is caused by the stirring of the magnetic bar.

The enzyme electrode is distinguished by a fast response to the substrate. Chen and others used a sol-gel-derived electrode doped with Eastman AQ polymer in order to meet with a fast response time ($t_{95\%}$ = 20 sec) and claim they can process sixty or more samples per hour [33,34]. Figure 5(b) shows the signal of our rose electrode to be saturated within 20 second approximately. This is highly dependent on the rotational frequency of the magnetic stirrer.

Figure 6 is a Hanes-Woolf plot obtained by taking the reciprocals of accumulative signals with the substrate concentrations in Figure 5(a). The linearity of Hanes-Woolf plot indicates that the reaction is enzyme-catalytic. The plot shows good linearity with the correlation of 0.998. This implies the electrolysis of hydrogen peroxide is catalyzed by the enzyme in the system. From this, $K_M = 8.8 \times 10^{-4}$ M and $i_{max} = 5.0 \times 10^{-7}$ A.

Figure 7 shows the current response in the double-step chronoamperometry at 0.01 M substrate concentration. This is an optimum technique to show whether the system is reversible or not. As shown

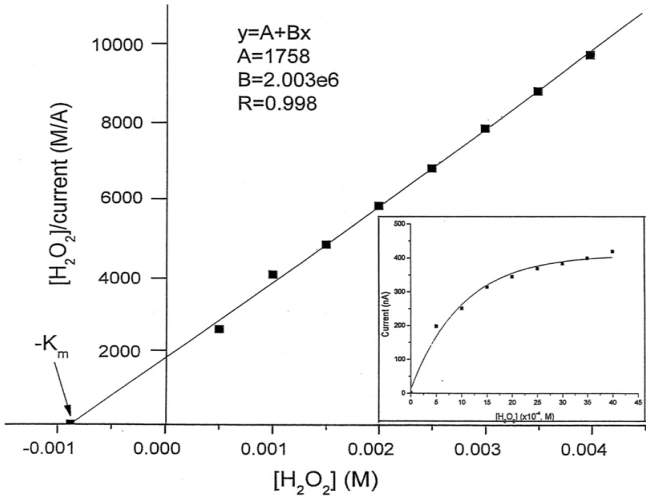

Figure 6. Hanes-Woolf plot for enzyme kinetics. Inset : the calibration curve elicited from Figure 5(a).

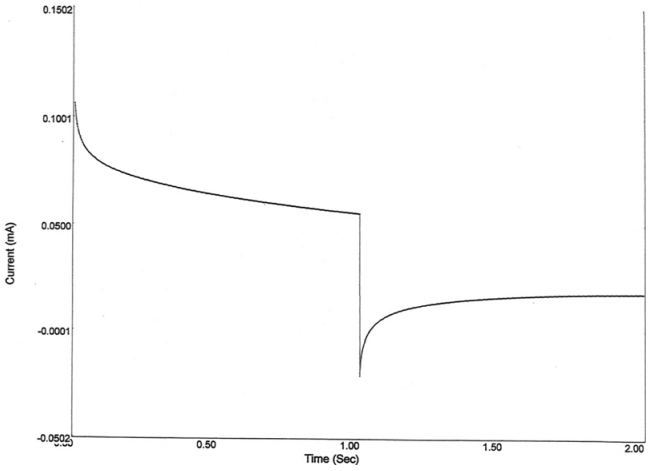

Figure 7. Current profile obtained by the double step technique. Start potential : 0 (mV); first step E : -200 (mV); second step E : 0.00 (mV). [H_2O_2] : 0.01 M ; [NaCl] : 1.0 × 10^{-3} M.

Table 3. Time Profile of the Observed and the Theoretical $-i_r/i_f$. t_f and t_r are the sampling times in the forward (i_f) and the reversal step (i_r) respectively. $t_f = t_r - \tau$ ($\tau = 1$)

t_f (× 10^{-3}, sec)	1.0	2.0	3.0	4.0	5.0	6.0	7.0	8.0
$i_{f,\ tf}$ (mA)	0.1055	0.1026	0.1020	0.1002	0.0990	0.0978	0.0973	0.0967
$i_{r,\ tr-\tau}$ (mA)	-0.022	-0.019	-0.016	-0.015	-0.013	-0.012	-0.011	-0.010
$-i_r/i_f$	0.21	0.19	0.16	0.15	0.13	0.12	0.11	0.10
$1-(1-\tau/t_f)^{1/2}$	0.97	0.96	0.95	0.94	0.93	0.92	0.92	0.91

in Figure 1, the first step potential, -200 mV, is enough to reduce the substrate and the second step potential, 0.00 mV, the lowest in the experimental range of the electrode potential. The forward current, i_f and the reversal current, i_r, which were sampled at t_f during the first step and at $t_f + \tau$ (τ = 1 sec) during the reversal step respectively, are given in Table 3. When H_2O_2 is electrochemically reduced, the product is solvent, H_2O, which exists to an unlimited extent in this system. Accordingly the real experiment, $-i_r/i_f$ should be in accordance with the theoretical values predicted in case of $1-(1-\tau/t)^{1/2}$, for a totally reversible cathodic reaction. Figure 8 shows a wide difference between the two. Various other readings are possible.

Significantly, $(-i_r/i_f)/\{1-(1-\tau/t)^{1/2}\}$ is 0.25 at $t_r/\tau = 1$ and all values of $-i_r/i_f$ fall between 0.11 and 0.25 in the full scope of t_r/τ. Taking the residual current formed during the reversal step into consideration, it is obvious that the reversible current is extremely small or non-existent. Therefore, it is possible to conclude that the redox reaction of substrate is totally irreversible in this system.

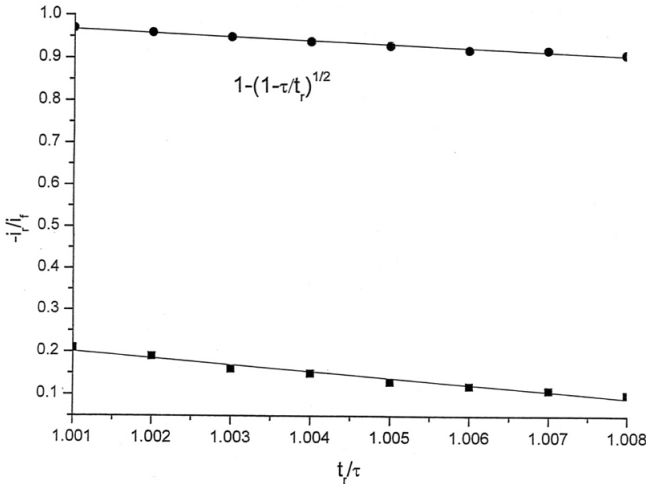

Figure 8. Working curve for $-i_r/i_f$ elicited from Figure 7.

4. Conclusion

The above results demonstrate that the rose electrode functions as a hydrogen peroxide biosensor quantitatively. This proves that the rose leaf embedded carbon paste electrode is ready to be put to practical use. The electrode bound with the rubber solution exhibited a mechanical hardness after the evaporation of solvent and was a semipermanent instrument for the determination of hydrogen peroxide. But its ability to sense substrate degenerates with long use, even though it is a common event in most enzyme electrodes. This drawback seems to arise from the thermal denaturation of enzyme protein in normal room conditions. Therefore, further research is required for lengthening the shelf life of the electrode.

Acknowledgements

This study was supported by a research grant (special project) in

2013～2014 from Cheongju University.

References

1. I. Sax, Hawley's Condensed Chemical Dictionary, 168, Van Nostrand Reinhold, NY, USA (1987).
2. J. Wang, H. Ye, Z. Jiang, and J. Huang, Determination of diethylstilbestol by enhancement of luminol-hydrogenperoxide-tetrasulfonated cobalt phthalocyanine chemiluminescence, *Anal. Chim. Acta*, **508**, 171-176 (2004).
3. B. Tang and Y. Wang, Spectrofluorimetric determination of both hydrogen peroxide and -O-O-H in polyethylene glycols (PEGs) using-2-hydroxy-1-naphthaldehyde thiosemicarbazone (HNT) as substrate for horseradish peroxidase (HRP), *Spectrochim. Acta, Part A*, **59**, 2867-2874 (2003).
4. S. Svensson, A. C. Olin, M. Lärstad, G. Ljungkvist, and K. Torén, Determination of hydrogen peroxide in enhaled breath condensate by flow injection analysis with fluorescence detection, *J. Chromatogr. B*, **809**, 199-203 (2004).
5. E. Casero, M. Darder, F. Pariente, and E. Lorenzo, Peroxidase enzyme electrodes as nitric oxide biosensors, *Anal. Chim. Acta*, **403**, 1-9 (2000).
6. W. Zwirtes de Oliveira, and I. C. Vieira, Immobilization procedures for the development of a biosensor for the determination of hydroquinone using chitosan and glio (salanum glio), *Enzyme Microb. Technol*., **38**, 449-456 (2006).
7. S. Tingry, C. Innocent, S. Touli, A. Deratani, and P. Seta, Carbon paste biosensor for phenol detection of impregnated tissue: modification of selectivity by using β-cyclodextrin-containing PVA membrane, *Mater. Sci. Eng. C*, **26**, 222-226 (2006).
8. J. Wang, J. W. Mo, S. F. Li, and J. Porter, Comparison of oxygen-rich and mediater-based glucose-oxidase carbon-paste electrodes, *Anal. Chim. Acta*, **441**, 183-189 (2001).
9. E. Crouch, D. C. Cowell, S. Hoskins, R. W. Pitsson, and J. P. Hart, Amperometric, screen-printed, glucose biosensor for analysis of human plasma samples using a biocomposite water-based carbon inc incorporating glucose oxidase, *Anal. Biochem*., **347**, 17-23 (2005).
10. F. M. Tian, B. Xu, L. D. Zhu, and G. Y. Zhu, Hydrogen peroxide biosensor with enzyme entrapped within electrodeposited polypyrrole based on mediated sol-gel derived composite carbon electrode, *Anal. Chim. Acta*, **443**, 9-16 (2001).
11. S. Gaspar, K. Habermüller, E. Csöregi, and W. Schuhmann, Hydrogen peroxide sensitive biosensor based on plant peroxidases entrapped on Os-modified polypyrrole films, *Sens. Actuators B*, **72**, 63-68 (2001).
12. T. J. Cheng, T. M. Lin, and H. C. Chang, Physical adsorption of protamine for heparin assay using a quartz crystal microbalance and electrochemical impedance spectroscopy, *Anal. Chim. Acta*, **462**, 261-273 (2002).
13. J. J. Wang and M. S. Lin, Horseradish-root-modified carbon paste electrode, *Electroanalysis*, **1**, 43-48 (1989).
14. H. Horie and G. A. Rechnitz, Hybrid tissue/enzyme biosensor for pectin, *Anal. Chim. Acta*, **306**, 123-127 (1995).
15. H. S. Kwon, I. K. Park, K. J. Yoon, and M. L. Seo, Plant tissue-based amperometric sensor for determination of phenols in methylene chloride, *J. Kor. Chem. Soc*., **44**, 376-379 (2000).
16. B. G. Lee, K. J. Yoon, and H. S. Kwon, Spinach root-tissue based amperometric biosensor for the determination of hydrogen peroxide, *Anal. Sci. Tech*., **13**, 315-322 (2000).
17. K. J. Yoon, Optimum pH of the reduction of hydrogen peroxide at a tobacco plant tissue based amperometric biosensor, *J. Kor. Chem. Soc*., **48**, 654-658 (2004).
18. H. S. Kwon, E. H. Jin, K. J. Yoon, and Y. N. Pak, Mushroom-juice based gold electrode for the determination of phenols, *J. Kor. Chem. Soc*., **49**, 224-228 (2005).
19. B. G. Lee, S. W. Park, and K. J. Yoon, Electrochemical properties of the mugwort-embedded biosensor for the determination of hydrogen peroxide, *Anal. Sci. Tech*., **19**, 58-64 (2006).
20. H. S. Kwon, H. J. Kim, K. J. Yoon, and Y. N. Pak, Chard root-tissue based biosensor for the determination of dopamine, *J. Kor. Chem. Soc*., **51**, 291-297 (2007).
21. K. J. Yoon, S. Y. Pyun, and H. S. Kwon, Chicken liver tissue-based amperometric biosensor for the determination of hydrogen peroxide, *J. Kor. Chem. Soc*., **41**, 343-350 (1997).
22. K. J. Yoon, Electrochemical Investigation of Animal Tissue Embedded Biosensor Bound with Ethylene-Propylene Rubber, *Bull. Kor. Chem. Soc*., **31**, 2913-2917 (2010).
23. H. S. Dho and K. J. Yoon, Electrochemical kinetic study of amperometric hydrogen peroxide biosensor fabricated using SBR, *J. Ind. Eng. Chem*., **17**, 254-258 (2011).
24. J. A. Brydson, Rubbery materials and their compounds, 291, Elsevier Applied Science, London and New York (1998).
25. A. Mansouri, D. P. Makris, and P. Keflas, Determination of hydrogen peroxide scavenging activity of cinnamic and benzoic acids employing a highly sensitive peroxyoxalate chemiluminescence-based assay, *J. Pham. Biomed. Anal*., **39**, 22-26 (2005).
26. R. F. P. Nogueria, M. C. Oliveira, and W. C. Paterlini, Simple and fast spectrophotometric determination of H_2O_2 in photo-fenton reactions using metavanadate, *Talanta*, **66**, 86-91 (2005).
27. E. Graft, J. R. Mahoney, R. G. Bryant, and J. W. Eaton, Iron-catalyzed hydroxyl radical formation, *J. Biol. Chem*., **259**, 3620-3624 (1984).
28. E. S. Henle, and S. Linn, Formation, prevention, and repair of DNA damage by iron/hydrogen peroxide, *J. Biol. Chem*., **272**, 19095-19098 (1997).
29. K. J. Yoon. A new strategy for determining optimum pH of isozymes, *Bull. Kor. Chem. Soc*., **25**, 997-1002 (2004).
30. K. J. Yoon, Electrochemical Studies on the voltammetric characteristics of hydrogen peroxide biosensor immobilized by natural rubber, *J. Kor. Chem. Soc*., **52**, 197-202 (2008).
31. A. N. Díaz, M. C. R. Peinado, and M. C. T. Minguez, Sol-gel horseradish peroxidase biosensor for hydrogen peroxide detection by chemiluminescence, *Anal. Chim. Acta*, **363**, 221-227 (1998).
32. Y. H. Yang, M. H. Yang, H. Wang, L. Tang, G. L. Shen, and R. Q. Yu, Inhibition biosensor for determination of nicotine, *Anal. Chim. Acta*, **509**, 151-157 (2004).
33. X. Chen, J. Z. Zhang, B. Q. Wang, G. J. Cheng, and S. J. Dong, Hydrogen peroxide biosensor based on sol-gel-derived glasses doped with Eastman AQ polymer, *Anal. Chim. Acta*, **434**, 255-260 (2001).